Long Non-coding RNA CBR3-AS1 Mediates Tumorigenesis and Radiosensitivity of Non-small Cell Lung Cancer through Redox and DNA Repair by CBR3-AS1 /miR-409-3p/SOD1 Axis

Shilong Liu (113897922@qq.com)
Harbin Medical University
Ning Zhan
Xiang'an Hospital of Xiamen University
Chunzi Gao
The First Affiliated Hospital of Harbin medical university
Piao Xu
Xiang'an Hospital of Xiamen University
Hong Wang
school of ophthalmology and optometry and eye hospital,school of biomedical engineering,wenzhou medical university
Siyu Wang
Harbin Medical University Third Hospital: Tumor Hospital of Harbin Medical University
Shiqi Piao
Harbin Medical University Third Hospital: Tumor Hospital of Harbin Medical University
Suwei Jing
Harbin Medical University Third Hospital: Tumor Hospital of Harbin Medical University

Research

Keywords: NSCLC, CBR3-AS1, miR-409-3p, SOD1, radiosensitivity, ROS

Posted Date: July 20th, 2021

DOI: https://doi.org/10.21203/rs.3.rs-703986/v1

Abstract

Background: Long noncoding RNA (lncRNA) CBR3-AS1 has important functions in various cancers. However, the biological functions of CBR3-AS1 in non-small lung cancer (NSCLC) remains unclear. This study aimed to investigated the roles and molecular mechanisms of lncRNA CBR3-AS1 in NSCLC tumorigenesis and radiosensitivity.

Methods: The association of CBR3-AS1 expression with the clinicopathological features and prognosis of NSCLC was studied based on The Cancer Genome Atlas database and verified in tumor and adjacent normal tissues of 48 NSCLC patients. The effect of CBR3-AS1 knockdown or overexpression on proliferation, apoptosis, migration, and invasion of NSCLC cells were studied through CCK-8, flow cytometry, and transwell assays, and tumorigenesis experiments in nude mice. The interactions of CBR3-AS1, miR-409-3p, and SOD1 were investigated using double luciferase reporter gene. The effect of CBR3-AS1 on NSCLC radiosensitivity was verified using clone formation assay and the single-click multi-target mathematical model. Changes in γH2AX level and reactive oxygen species (ROS) levels were detected using immunofluorescence and flow cytometry in NSCLC cells after irradiation.

Results: CBR3-AS1 expression in NSCLC tissue was increased significantly compared with that of surrounding normal tissue. Cell function experiments verified that CBR3-AS1 downregulation could reduce proliferation, invasion, and migration of NSCLC cells and inhibit cell cycle progression and promote apoptosis. The tumorigenesis experiment in nude mice showed that CBR3-AS1 promoted tumor growth. CBR3-AS1 could regulate the expression and functions of the target gene SOD1 of miR-409-3p. High CBR3-AS1 expression in NSCLC was negatively correlated with radiosensitivity. CBR3-AS1 downregulation in NSCLC may depress the expression of SOD1 after irradiation, promote the formation of γH2AX, increase levels of ROS, and increase apoptosis.

Conclusions: CBR3-AS1 is highly expressed in NSCLC, and play oncogene function through the CBR3-AS1/miR-409-3p/SOD1 pathway. Downregulation of CBR3-AS1 led to enhanced radiosensitivity, thus providing a new therapeutic target for NSCLC.

Background

Lung cancer include two major types: small cell lung cancer (SCLC) and the non-small cell lung cancer types (NSCLC), NSCLC mainly includes two pathological types: adenocarcinoma and squamous cell carcinoma. Although the incidence and mortality rates of lung cancer have been significantly reduced through smoking cessation programs and therapeutic advances, the prognosis of non-small cell lung cancer (NSCLC) is still poor, with a five-year overall survival (OS) rate of only 26% [1]. Contributory factors include late-stage disease at the time of initial presentation, tumor resistance, and patient intolerance of radiotherapy and so on. Therefore, to improve diagnostic capabilities, reduce radioresistance, prolong survival, and improve prognosis, it is particularly important to study NSCLC pathogenesis and radioresistance mechanisms.

Long non-coding RNAs (lncRNAs) are RNA segments with lengths of over 200 nt that do not encode proteins, but have important biological functions through interactions with target DNAs, RNAs, and proteins during gene expression, cell growth, and differentiation [2]. Abnormal lncRNA expression plays a key role in the pathogenesis of numerous diseases including genetic disorders, diabetes, and cancer [3]. LncRNAs can regulate gene expression levels and are involved in multiple cellular activities by regulating tumor formation, apoptosis, cell proliferation, invasion and migration radioresistance [3–5].

CBR3-AS1, also known as plncRNA-1, is a lncRNA encoded on chromosome 21q22.12 with a transcriptional length of 749 nt and was initially found to be highly expressed in prostate cancer tissues and cells [6]. CBR3-AS1 has been confirmed as an oncogene in a variety of malignant tumors. CBR3-AS1 knockdown in prostate cancer cells can inhibit tumor cell proliferation and promote apoptosis by regulating androgen expression [7, 8]. Previous studies have demonstrated that CBR3-AS1 is highly expressed and associated with lymphatic metastasis and poor prognosis in esophageal cancer [9]. Zhang et al. found that high CBR3-AS1 expression was an independent adverse prognostic indicator in patients with osteosarcoma. CBR3-AS1 knockdown can reduce proliferation, migration, and invasiveness, and can promote apoptosis of osteosarcoma cells [10]. In addition, CBR3-AS1 can promote epithelial-mesenchymal transition and metastasis of hepatoma cells [11]. However, to our knowledge, the functional role of CBR3-AS1 in NSCLC have not been reported.

MicroRNAs (miRNAs) are noncoding RNA segments with sequence lengths of 18 to 25 nt that bind to specific sites from the 3' end of the translation sections of target mRNAs (3' UTR) in transcriptional or post-transcriptional regulation of gene expression, resulting in degradation or inhibition of transcription and translation [12]. MiRNA expression is involved in multiple physiological and pathological processes, including cell differentiation, development, proliferation, apoptosis, and tumorigenesis [13]. MiR-409-3p expression was initially described in embryonic stem cells in vivo [14]. As a tumor suppressor gene, miR-409-3p is underexpressed in a variety of malignant neoplasms, such as breast and bladder cancers [15, 16]. Currently, there are few reports on the function of miR-409-3p expression in NSCLC. Wan et al. found that miR-409-3p was significantly downregulated in lung adenocarcinoma tissue compared with adjacent normal tissues, inhibited the growth, migration, and invasion of tumor cells, furthermore, it could target c-Met to inactivate the Akt signal, thereby inducing apoptosis [17]. Our previous study confirmed that miR-409-3p was significantly low-grade expressed in NSCLC cells and tissues [18].

Superoxide dismutase (SOD) functions in numerous cell types to scavenge superoxide anion free radicals and convert superoxide to oxygen and hydrogen peroxide. There are three SOD subtypes: SOD1, SOD2 and SOD3. SOD1 (copper/zinc superoxide dismutase) is the predominant active form, accounting for 80% of intracellular SOD activity [19]. Although SOD1 is located primarily in the cytoplasm, it is also distributed in the nucleus and mitochondrial membrane space. SOD2 and SOD3 function similarly to SOD1, but are located in different cellular substructures. During oxidative stress, SOD1 can maintain a low superoxidation level to protect cancer cells or other cells with abnormal functions from oxidative injury and death [19–21]. SOD1 gene mutations are associated with many human cancers, especially NSCLC [20]. Somwar et al. reported SOD1 overexpression in lung adenocarcinoma compared with normal

lung tissue, and concluded that SOD1 can promote lung cancer cell proliferation and inhibit apoptosis [21]. Glasauer et al. found that ATN-224, a small molecule inhibitor of SOD1, can induce NSCLC cell death [22]. Our previous study confirmed that SOD1 was highly expressed in NSCLC cells and tissues, and found that SOD1 overexpression promoted proliferation, migration, and invasion of NSCLC cells, and was an independent indicator of poor prognosis in NSCLC patients [18]. Moreover, radioresistance in esophageal cancer cells has been associated with upregulated SOD1 expression [23].

Herein, we found that CBR3-AS1 overexpression could significantly reduce survival, increase NSCLC cell proliferation, facilitate migration and invasion, promote cell cycling, inhibit apoptosis and elevate radioresistance. Furthermore, we confirmed that CBR3-AS1 can act as a ceRNA to regulate the expression and function of the miR-409-3p target gene SOD1 in NSCLC. Our results demonstrated that CBR3-AS1 might be a new therapeutic targets and diagnostic markers for NSCLC, and a potential target for radiosensitization.

Materials And Methods

Cell lines, animal care, and clinical tissue specimens

Cell lines

NSCLC cell lines A549, H1650, H520, H460, H1299, PC9, and the human normal bronchial epithelial cell line 16HBE were purchased from the Cell Bank of the Chinese Academy of Sciences (Shanghai), and our laboratory was entrusted to conduct related culture and passage work. The aforementioned cell lines were cultured as adherent cells, using either L - glutamine DMEM media culture PC9 for human bronchial epithelial cells, or RPMI − 1640 medium for all other cells, each supplemented with 100 u/mL penicillin and streptomycin, and 10% fetal bovine serum. All cultures were performed using a conventional ultraclean technique, with cells in volume fraction, and incubated at 37 ℃ in a 5% CO_2 atmosphere with saturated humidity.

Nude mice

Nude mice were obtained from the Animal Experimental Center of the Second Affiliated Hospital of Harbin Medical University. The mice were reared in cages at a room temperature of 22 ± 2°C, 60 ± 5% humidity, and constant ventilation.

Tissue

Our study was conducted at the Affiliated Tumor Hospital of Harbin Medical University from June 2016 to January 2017, with the approval of the Medical Ethics Committee. Surgical specimens containing cancerous and paracancerous tissues were obtained with the informed consent of the patients and their

families from 48 patients undergoing resection of NSCLC. None of the selected patients had received preoperative antitumor therapy. Fresh surgical specimens were placed in liquid nitrogen containers for cryopreservation within 5 minutes after excision, while those requiring long-term preservation were transferred to an -80℃ environment.

Cell transfection

The SiRNA used in this study was designed and synthesized by the Shanghai Invitrogen Company, and is shown in Table 1. Lipo2000 was used for transfection.

Table 1
Oligonucleotides used in the study of CBR3-AS1

Gene	Orientation	5'- 3' primer sequence
siRNA-1	Forward	GGACAGUGAAGAACAGGAUTT
	Reverse	AUCCUGUUCUUCACUGUCCTT
siRNA-2	Forward	CCAGGAUGUAAUCCAGCUUTT
	Reverse	AAGCUGGAUUACAUCCUGGTT
siRNA-3	Forward	GGUCACAUAAGUUUGGCAATT
	Reverse	UUGCCAAACUUAUGUGACCTT
siRNA-NC	Forward	UUCUCCGAA CGU GUC ACG UTT
	Reverse	ACGUGA CAC GUU CGG AGA ATT
miR-409-3p inhibitor	Forward	GAATGTTGCTCGGTGA
	Reverse	GTGCAGGGTCCGAGGT
U6	Forward	GCTTCGGCAGCACATATACT
	Reverse	GTGCAGGGTCCGAGGTATTC
GAPDH	Forward	GCACCGTCAAGGCTGAGAC
	Reverse	TGGTGAAGACGCCAGTGGA
SOD1	Forward	CTGAAGGCCTGCATGGATTC
	Reverse	CCAAGTCTCCAACATGCCTCT

Lentivirus transfection

The full-length cDNA sequences of lncRNA CBR3-AS1, the miR-409-3p mimic 5'-gaauugugcucggugaacccu-3', the SOD1 5'-tcccttggatgtagtctgaggactccatt-3', and the negative control sequence 5'-actgagtgcagtaga-3' were constructed on pLVX-Puro lentivirus expression vectors. The

enzyme digestion sites used were KpnI and XhoI, which were completely consistent with the sequence BLAST on NCBI after sequencing. This step was assisted by Beijing Qingke Xinye Biotechnology Co, Ltd. The map of lentiviral expression vector pLVX-Puro is shown in Fig. 1A.

Cell irradiation

Cell culture dishes were sealed before radiotherapy to prevent contamination. Cells were irradiated with 6MV X beams from a distance of 100cm and at a dose rate of 400cGy/min.

RNA extraction and real-time fluorescence quantitative PCR

Tissue total RNA was extracted by the Trizol method, using a nucleoplasmic separation and extraction kit. U6 and GAPDH were used as internal references in the nucleus and cytoplasm, respectively. PCR amplification was carried out by Roche FastStart™ Universal Sybr® Green Master, and the target gene content was detected by the ABI PRISM™ 7500 fluorescent quantitative PCR amplification instrument. The procedure has been described in detail previously [18].

Western blot

Specific steps of the Western blot procedure have been described previously [18].

Cell proliferation

Cell proliferation assays were conducted by using a CCK-8 proliferation-toxicity detection kit (Tongren, Japan), according to the manufacturer's instructions. Changes of NSCLC cell proliferation after CBR3-AS1overexpression and knockdown were evaluated. H520 cells were transfected with siRNA-CBR3-AS1 at 0 h, 24 h, 48 h and 72 h, and optical density values at the wavelength of 450nm were detected in the following 2 hours. Specific steps have been described previously [18].

Cell invasion and migration assays

Transwell assays were used to measure cell invasion and migration as described previously [18].

Flow cytometry

Cell cycle and apoptosis were determined by using the BD FACSCANTO™ II flow cytometer, according to the instructions of the BD cell cycle kit and the FITC Annex V Apoptosis Detection Kit I reagent box, as shown previously [18].

Detection of intracellular total reactive oxygen species (ROS)

The effect of CBR3-AS1 on the radiosensitivity of NSCLC cells by regulating ROS levels was investigated. ROS were labeled with a 2, 7-dichlorofluoresce yellow diacetate (DCFH-DA) probe. DCFH-DA probes enter the cell freely through the cell membrane and were oxidized by intracellular ROS to form ethyl oxide. Ethyl oxide is incorporated into chromosomal DNA to produce red fluorescence that can be assayed to determine cellular ROS content. The changes of ROS levels before and after irradiation were detected by a

loss cell analyzer. After adherent cell growth, logarithmic-phase cells were inoculated in 6-well plates and exposed to 6MV X beam radiation, then using DCFH-DA probes (1:500 dilution) illuminated after 1, 2, 3, 4, 5, and 6 hours. Then, cells were incubated at room temperature without light for 20 min, PBS was used to clean and collect digestive cells, and fluorescence intensity of each sample at 480nm was analyzed by flow cytometry.

Double luciferase reporter assay

The miRNAs and potential CBR3-AS1 binding sites were analyzed by starBase v3.0 bioinformatics software. The corresponding pmiR-RB-luciferase reporter vector (Promega, USA) was constructed by using the Quick Change Lighting kit (Stratagene, La Jolla, CA, USA), as described previously [18].

Tumor formation experiment in nude mice

After the encoding plasmid was expressed stably, 200 μL(5×107) CBR3 - AS1-overexpressing H1650 cell and control H1650 cell suspensions were injected into the subcutaneous tissue of the outer abdominal wall of nude mice, and the subcutaneous tumor growth was observed regularly. Short (A) and long (B) tumor diameters were measured with a vernier caliper. Four weeks later, the mice were humanely euthanized, tumor tissues were removed, the volume and mass of tumors were measured and photographed. Tumor volumes were calculated by the formula $V = 1/2 \times A \times B^2$, and the tumor growth curve was derived.

Immunofluorescence

Double-stranded DNA rupture that causes DNA double-stranded breaks (DSBs) is the primary mechanism of cell damage and death induced by ionizing radiation. DSBs provoke phosphorylation of serine at site 139 of histone H2AX to quickly, which raises other signaling molecules and triggers a cascade to repair DSBs. Because γH2AX is closely related to DSBs, testing double-stranded DNA has become primary assay to measure DNA repair ability. In this study, γH2AX focal points in NSCLC cells at different time points after irradiation were detected by immunofluorescence technique, and the effect of CBR3-AS1 on DSBs of NSCLC cells induced by ionizing radiation was observed.

Logarithmic growth phase cells were inoculated into a petri dish. After cells were firmly attached to the vessel wall (24 h), 4Gy X rays were given. 1h after irradiation, cells were exposed to 4% paraformaldehyde containing 0.2% of Triton X − 100 for 30min, followed by cellular rupture in solution. The H2AX rabbit polyclonal anti-human antibody, horseradish peroxidase, and goat anti-rabbit antibody were added after 1h to the petri dish with 2 g/mL DAPI, and allowed to stand at room temperature for 15 min. The focal points of γ-H2AX were observed and photographed by laser confocal microscopy.

Clone formation

Cell suspensions were diluted by multiple gradients. Radiation dose points of 0, 2, 4, 6, and 8Gy were delivered by 6MVX beams to gradient densities of 100, 200, 400, 1000 and 2000 cells. Cell suspensions were then incubated at 37°C for 10–14 days. When clones were grossly visible, the culture was stopped,

and crystal violet fixation solution was added for 45 minutes. Clones of more than 50 cells were counted under microscopy. Survival scores were tallied using the following formulas:

Platting efficiency (PE) = number of clones formed in control group/number of inoculated cells ×100%.

Survival fraction (SF) = [number of clones/(number of inoculated cells × PE)] × 100%.

The abscissa was set as dose and the ordinate was set as survival rate. By using the single-click multi-target mathematical model Y = 1-[1-exp(-d /D0)]^N [24] for formula fitting, the cell survival curve in the semi-logarithmic coordinates of the cell line could be obtained as the cell dose-effect curve.

Radiosensitivity test

To determine the effect of CBR3-S1 on the radiosensitivity of NSCLC cells, a plate clone formation assay was used to detect the clone formation rates of H520 cells transfected with si-CBR3-AS1 and H1650 cells transfected with pLVX-Puro-CBR3-AS1 after irradiation with doses of 0Gy, 2Gy, 4Gy, 6Gy and 8Gy. A single target multi-strike model was used to fit the survival curves of different experimental groups, and radiobiological parameters such as D0, DQ, N and SF2 were calculated and analyzed. These parameters have been widely used in the assessment and analysis of radiosensitivity, and can reflect the radiobiological characteristics of cells comprehensively and accurately. Wherein, K is the cell passivation constant, and N is the extrapolated value, the intercept of the curve index extending to the Y axis intersection theoretically represents the number of intracellular targets and can reflect the cellular capacity to repair radiation damage. K and N values can be given directly by the fitting survival curve. D0 is the average lethal dose, which is the dose required to reduce the index region of the curve by 63%, and is the reciprocal of the slope of the straight part of the survival curve, that is, D0 = 1/K. Theoretically, D0 is the average dose required to radiate each cell once. The DQ quasi-threshold dose is estimated by drawing a line parallel to the horizontal axis and beyond the vertical axis 1.0 point. Its point intersection with the extrapolation line projected to the horizontal axis value represents the survival curve "shoulder width" that represents the cellular sublethal injury. The ability of the cell to repair the sublethal injury is calculated by Dq = D0×ln (N). SF2 refers to the survival fraction (theoretical value) of cells irradiated by 2Gy rays. D0, DQ, the values of N and SF2, the greater the cell radiation resistance stronger, by means of fitting curve of survival at the same time. We performed value calculations of radiosensitivity by using sensitization enhancement ratio: D0 (control group)/D0 (experimental group).

Statistical analysis

Experimental data were analyzed by SPSS21.0 and GraphPad Prism Version 6.0. The mean ± standard deviation of the results of three independent experiments were uniformly selected for experimental data. The independent sample t test was used for the comparison between two samples. The Chi-Square test was used for the analysis of clinical characteristics, and the Kaplan-Meier method, the Log-rank method, and the Cox regression risk factor model were used to analyze survival prognosis. To evaluate the relationship between clinicopathological features and CBR3-AS1 expression level, we conducted a correlation analysis. $P < 0.05$ indicated statistically significant differences.

Results

CBR3-AS1 expression in NSCLC and its relationship with clinicopathological features

We extracted lncRNAseq information from the TCGA database using bioinformatics technology and analyzed all CBR3-AS1-related data. Screening for abnormal lncRNA expression in NSCLC showed that CBR3-AS1 was significantly overexpressed in both squamous cell and adenocarcinomas of the lung ($P < 0.001$, Fig. 1B). Moreover, the ratio of high CBR3-AS1 expression in lung adenocarcinoma was significantly greater than that of lung squamous cell carcinoma ($P < 0.001$, Fig. 1B). Further analysis verified that CBR3-AS1 expression in NSCLC surgical specimens was significantly higher than that in the corresponding normal tissues ($P < 0.05$, Fig. 1C-D). qRT-PCR disclosed increased CBR3-AS1 expression in the H520, H460, PC9 and A549 NSCLC cell lines compared to controls ($P < 0.05$, Fig. 1E). The TCGA database also was used to detect the prognostic significance of NSCLC CBR3-AS1 expression, it showed that CBR3-AS1 was closely associated with poor prognosis ($P < 0.001$, Fig. 1F). Kaplan-Meier survival curves also demonstrated that OS and disease-free survival (DFS) of the patients with high CBR3-AS1 expression were significantly lower than those with low CBR3-AS1 expression ($P < 0.001$, Fig. 1G-H). Moreover, we investigated that CBR3-AS1 expression correlated with tumor size ($P < 0.001$), lymph node metastasis ($P < 0.05$), and a histopathologic diagnosis of adenocarcinoma ($P < 0.001$) (Table 2), and there were no significant correlations between CBR3-AS1 expression level and smoking, gender, and age ($P > 0.05$). The results indicated that CBR3-AS1 could predict the low prognosis of NSCLC.

Table 2
Association between CBR3-AS1 expression and clinicopathological characteristics of NSCLC patients

Variable	All patients (n = 48)	CBR3-AS1 expression		*P*
		High (%) (n = 34)	Low (%) (n = 14)	
Smoking				
Never	27	14 (41)	7 (50)	0.575
Ever	21	20 (59)	7 (50)	
Gender				
Male	26	18 (53)	8 (57)	0.791
Female	22	16(47)	6 (43)	
Age (years)				
< 65	37	27 (79)	10 (71)	0.550
≥ 65	11	7 (21)	4 (29)	
Differentiation				
Well	13	9 (26)	4 (28)	0.882
Moderate/ Poor	35	25 (74)	10 (72)	
Histological cell type				
Adenocarcinoma	25	22 (65)	3 (22)	0.006*
Squamous cell carcinoma	23	12 (35)	11 (78)	
pT classification				
T1/2	30	17 (50)	13 (93)	0.005*
T3/4	18	17 (50)	1 (7)	
Lymph node metastasis				0.021*
Present	19	17(50)	2 (14)	
Absent	29	17 (50)	12 (86)	

CBR3-AS1 promote the prolifetation, migration, invasion, cell cycle and apoptosis.

Subcellular localization assays disclosed that CBR3-AS1 was significantly overexpressed in cytoplasm ($P < 0.05$, Fig. 2A).

qRT-PCR disclosed that CBR3-AS1expression was highest in H520 NSCLC cells, and lowest in H1650 NSCLC cells (Fig. 1D). Consequently, we used siRNA technology to knock down CBR3-AS1 expression in H520 cells, and designed three siRNA strands, designated siRNA-1, siRNA-2 and siRNA-3. qRT-PCR results showed that siRNA-1 knockdown was the most efficient (Fig. 2B). Our subsequent experiments used siRNA-1 to knockdown CBR3-AS1 in H520 cells. In addition, H1650 cells were infected with a lentivirus expression vector and screened with puromycin to obtain a stable H1650C cell line with high CBR3-AS1expression.

The viability of siRNA-CBR3-AS1 group was reduced compared with the control group (H520NC), and proliferation was diminished (Fig. 2C). In contrast, the proliferation of H1650C cells that overexpressed CBR3-AS1 was increased significantly compared with the control group (Fig. 2D). The transwell assay determined that knockdown of CBR3-AS1 significantly reduced the migration and invasion of NSCLC cells (Fig. 2E). Conversely, after the overexpression of CBR3-AS1, the number of migratory and invasive NSCLC cells was significantly enhanced compared to H1650NC controls (Fig. 2F).

In addition, Flow cytometry revealed that after transfection with siRNA-CBR3-AS1, the proportion of S phase H520 cells was significantly reduced, while the proportion of G1 phase cells was significantly increased and the proportion of G2 phase cells was unchanged compared with the control group, indicating that CBR3-AS1downregulation blocked the G1 to S phase transition (Figs. 2G-H). After CBR3AS1 overexpression, the proportion of S phase H1650C cells increased significantly, while the proportions of G2 cells were significantly reduced, but the proportions of G1cells were unchanged respectively, compared to controls, it shows that after overexpression of CBR3-AS1, the G1/S phase block was lifted, but the block from S phase to G2 phase occurred (Figs. 2G-H). These results suggest that CBR3-AS1 stimulates NSCLC cells to enter the cell division phase. Flow cytometry also disclosed that early and late apoptosis of CBR3 - AS1 knockdown NSCLC cells significantly was increased (Figs. 2I-J). On the contrary, the apoptosis rates of NSCLC cells that overexpressed CBR3-AS1 were significantly reduced (Figs. 2I-J). The above results proved that CBR3-AS1 could enhance proliferation, migration, invision, cell cycling and apoptosis of NSCLC cells.

The expression of CBR3-AS1 promoted the growth of tumor in vivo

To verified the roles of CBR3-AS1 in vivo, we injected H1650C cells or H1650NC cells into nude mice. Interestingly, tumor volume and weight in the CBR3-AS1 overexpression group were significantly increased compared to controls (Figs. 3A-D), indicating that CBR3-AS1 expression can promote the growth and proliferation of NSCLC cells in vivo.

MiR-409-3p is a target of CBR3-AS1

The starBase v3.0 bioinformatics analysis were employed to screen the downstream target miRNAs. (Fig. 4A). Among them, miR-409-3p, which is closely related to lung cancer and significantly low in NSCLC, was negatively correlated with CBR3-AS1 (Fig. 4B). Consequently, we selected miR-409-3p as the target of further bioinformatics study and found that the CBR3-AS1 sequence has a possible miR-409-3p binding site (Fig. 4C). Therefore, we hypothesized that CBR3-AS1 acts as a ceRNA that binds miR-409-3p in a targeted manner. We used a double luciferase reporter gene experiment to test this hypothesis. CBR3-AS1-WT, mutated CBR3-AS1 reporter vector (CBR3-AS1-MUT), miR-409-3p mimic, and miR-409-3p inhibitor were co-transfected into H520 and H1650 cells. miR-409-3p mimic enhanced the luciferase activity of CBR3-AS1-WT but did not enhance the CBR3-AS1-MUT group, compared to the control group. In contrast, miR-409-3p inhibitor significantly declined luciferase activity of CBR3-AS1-WT but did not changed the CBR3-AS1-MUT group, compared to the control group (Fig. 4D-E).

We next assessed the expression level of miR-409-3p in NSCLC samples, miR-409-3p was significantly downregulated in NSCLC surgical specimens compared to adjacent normal tissue (Fig. 4F). Furthermore, miR-409-3p expression was negatively correlated with tumor size ($P = 0.015$), lymph node metastasis ($P = 0.008$) and smoking ($P = 0.039$) (Table 3). Kaplan-Meier survival curves of the miR-409-3p high- and low-expression groups (using the average value of miR-409-3p as the boundary) disclosed that the OS and DFS of patients with high miR-409-3p expression were significantly better than those with low miR-409-3p expression ($P < 0.001$), suggesting that miR-409-3p may function as a tumor suppressor gene, and that miR-409-3p and CBR3-AS1 have opposite functions in NSCLC (Fig. 4G-H).

Table 3
Association between miR-409-3p expression and clinicopathological characteristics patients with NSCLC

Variable	All patients (n = 48)	miR-409-3p expression		*P*
		High (%) (n = 24)	Low (%) (n = 14)	
Smoking				
Never	20	6 (25)	14(58.3)	0.039*
Ever	28	18 (75)	10 (41.7)	
Gender				
Male	26	16 (66.7)	10 (41.7)	0.147
Female	22	8(33.3)	14 (58.3)	
Age (years)				
< 65	37	15 (62.5)	13 (54.2)	0.909
≥ 65	11	9 (37.5)	11 (45.8)	
Differentiation				
Well	13	5 (20.8)	8 (33.3)	0.517
Moderate/ Poor	35	19 (79.2)	16(66.7)	
Histological cell type				
Adenocarcinoma	20	11(45.8)	9 (37.5)	0.770
Squamous cell carcinoma	28	13 (54.2)	15 (62.5)	
pT classification				
T1/2	30	13 (54.2)	4 (16.7)	0.015*
T3/4	18	11 (45.8)	20 (83.3)	
Lymph node metastasis				
Present	28	9 (37.5)	19 (79.2)	0.008*
Absent	20	15(62.5)	5 (20.8)	

Subsequently, we found significantly reduced miR-409-3p expression in multiple NSCLC cell lines compared to normal human epithelial cells (Fig. 4I). Then, qRT-PCR assay evaluated that miR-409-3p expression in si-CBR3-AS1-treated H520 cells was significantly increased (Fig. 4J). In contrast, the expression of miR-409-3p in H1650C cells was significantly lower than in H1650NC control cells (Fig. 4K). qRT-PCR was used to further investigate the potential interactions of CBR3-AS1 and miR-409-3p in NSCLC cells, the results also disclosed that CBR3-AS1 expression was significantly decreased in H520 cells

transfected with miR-409-3p mimic (Fig. 4L), and significantly increased in H1650 cells after transfection with miR-409-3p inhibitor compared with the control group (Fig. 4M). Our results suggest that CBR3-AS1 and miR-409-3p are mutually antagonistic in NSCLC.

To determine whether miR-409-3p inhibits the function of CBR3-AS1 in NSCLC cells, we sought to reverse-verify the effect of miR-409-3p on NSCLC proliferation, invasion and migration. We conducted 4 Cell lines which were divided into miR-409-3p mimic, pLVX-Puro-CBR3-AS1 (H1650C), miR-409-3p mimic + H1650C, and control groups. The CCK-8 cell proliferation assay disclosed that proliferation of NSCLC cells promoted following CBR3-AS1 overexpression and significantly abrogated by miR-409-3p mimic (Fig. 5A). The transwell assay revealed that CBR3-AS1 upregulation and miR-409-3pmimic mediated promotion and suppression of the migration and invasion respectively in co-transfected miR-409-3pmic/pLVX-Puro-CBR3-AS1 cells were partly rescued and reversed (Figs. 5B-E). To conclude, these findings forcefully validate that CBR3-AS1 could function as a ceRNA by directly binding to miR-409-3p in NSCLC cells.

CBR3-AS1 as a ceRNA to regulate SOD1 which is the target gene of miR-409-3p

Our previous research confirmed that SOD1 is regulated by miR-409-3p as its target gene. To determine whether CBR3-AS1 can influence SOD1 expression by regulating the expression of miR-409-3p, qRT-PCR and Western blot was used. It detected that SOD1 mRNA and protein expressions in H1650 cells were significantly lower in the miR-409-3p mimic group than in the control group. however, SOD1 expression in the H1650C + miR-409-3p mimic group was reserved (Figs. 5F-H), suggesting that CBR3-AS1 expression blocked the inhibitory effect of miR-409-3p on SOD1 expression. In contrast, SOD1 expression was significantly higher in the miR-409-3p inhibitor group than in the control group, but was abolished in the si-CBR3-AS1 + miR-409-3p inhibitor groups in H520 cells, suggesting that reducing CBR3-AS1 expression might reverse the promotion of SOD1 expression by the miR-409-3p inhibitor (Figs. 5I-K). These results support our hypothesis that CBR3-AS1, as a ceRNA, can bind miR-409-3p in a targeted manner, thereby antagonizing the inhibitory effect of miR-409-3p on its target gene SOD1.

CBR3-AS1 weakened radiosensitivity of NSCLC cells

Radiation clonogenic survival assay showed that IR treatment (0–8 Gy) led to a dose-dependent reduction of cell survival fractions in H520 cells transfected with CBR3-AS1 knockdown (Fig. 6A-D). Results are shown in Table 4 and Figs. 6A-D. The D0, Dq, N and SF2 values of H520 cells after CBR3-AS1 downregulation were 1.46Gy, 0.89Gy, 1.83 and 0.42, respectively, while the D0, Dq, N and SF2 values of the corresponding control group were 2.79Gy, 0.46Gy, 1.18 and 0.56, respectively, and the sensitization enhancement ratio was 1.91. In contrast, CBR3-AS1 overexpression induced the remarkable increment of survival fractions of H1650 cells when cells were exposed to the same dose of IR. The D0, Dq, N and SF2 values of H1650 cells after CBR3-AS1 overexpression were 2.03Gy, 1.07Gy, 1.70 and 0.54, respectively, while the D0, Dq, N and SF2 values of control cells were 1.16Gy, 1.02Gy, 2.41 and 0.38, respectively, and the sensitization enhancement ratio was 0.57.

Table 4
Radiobiological parameters of NSCLC cells under the control of CBR3-AS1

Cell line	D0(Gy)	Dq (Gy)	N	SF2	SER
si-CBR3-AS1	1.46	0.89	1.83	0.42	-
si-NC	2.79	0.46	1.18	0.56	1.91
pLVX-puro-CBR3-AS1	2.03	1.07	1.70	0.54	0.57
pLVX-puro-NC	1.16	1.02	2.41	0.38	-

Furthermore, flow cytometry disclosed that radiation-induced apoptosis was accelerated in the CBR3-AS1 knockdown group (Fig. 6E-F). In contrast, the apoptosis rate of the IR + H1650C group was significantly reduced compared to the IR + H1650NC control group (Fig. 6G-H).

In addition, as shown in Figs. 6I-J, γH2AX nuclear foci increased significantly in the si-CBR3-AS1 group after 1h of irradiation, rose gradually, and then gradually declined after approximately two hours. γH2AX foci also increased in control cells after irradiation, but to a significantly lower degree, suggesting a delay in DNA repair in the siCBR3-AS1 group. As shown in Fig. 6K-L, γH2AX foci in the H1650C group at peaked 1 h after irradiation, and then gradually decreased. The number of γH2Ax foci in the H1650C group was decreased significantly compared with the control group at each time point. The γH2AX foci disappeared at about 6 hours, but were still visible in the control group.

ROS expression was significantly increased in the si-CBR3-AS1 group, gradually rising to peak at approximately 2h post-irradiation, followed by a gradual reduction, and significantly exceeding the results of the control group at corresponding time points (Fig. 6M-N). The ROS in H1650C group peaked at 1h after ionizing radiation and then gradually decreased. The ROS expression levels at each time point were significantly reduced compared with the control group (Figs. 6O-P). In a word, these data suggested that the radiosensitivity of NSCLC cells was significantly increased by reducing survival fractions, promoting apoptosis, delaying DNA repair and raising ROS level after CBR3-AS1 downregulation, but CBR3-AS1 overexpression significantly increased the radioresistance of NSCLC cells.

CBR3-AS1 knockdown potentiated NSCLC radiosensitivity through the CBR3-AS1/miR-409-3p/SOD1 pathway

To further determine whether CBR3-AS1 can function as a ceRNA to regulate SOD1 expression through miR-409-3p during irradiation, thus affecting the radiosensitivity of NSCLC cells. The expression of SOD1 mRNA and protein in the IR + si-CBR3-AS1 group was significantly lower than controls, while SOD1 mRNA and protein expression in the IR + si-CBR3-AS1 + miR-409-3p inhibitor group were higher than those of the IR + si-CBR3-AS1 group and was similar to the control group (Figs. 7A-B). Clone formation results (Fig. 7C-D) showed that the D0, Dq, n and SF2 values of the si-CBR3-AS1 + miR-4093p inhibitor group were 2.52 Gy, 0.30Gy, 1.13 and 0.63, respectively. The values of D0, Dq, n and SF2 in the si-CBR3-AS1 group were 1.46Gy, 0.89Gy, 1.83 and 0.47 respectively, while those in the corresponding control group were 2.79 Gy,

0.46 Gy, 1.18 and 0.56 respectively. Compared with si-CBR3-AS1 group, the sensitization enhancement ratio of the si-CBR3-AS1 + miR-4093p inhibitor group was 0.58, indicating that miR-409-3p expression was inhibited and that the radiosensitivity of the si-CBR3-AS1 group was consequently reduced. Taken together, CBR3-AS1 knockdown enhanced radiosensitivity by regulating miR-409-3p / SOD1 in NSCLC cells.

Discussion

A growing number of lncRNAs have been identified recently. Their expressions are usually tissue-specific [25]. They regulate gene expression through one or more of several mechanisms that include the induction of chromatin remodeling, transcriptional interference, the regulation of alternative splicing, and the alteration of protein localization or activity (such as scaffolding) in the assembly of multiple protein complexes [26].

Tumorigenesis and progression are results of gene expression disorders, usually involving the activation of oncogenes or the inactivation of tumor suppressor genes. LncRNAs, which can function as both oncogenes and tumor suppressor genes, may become future biomarkers and consequential therapeutic targets in the clinical management of lung cancer patients.

Carcinogenic lncRNAs that promote the growth of cancer cells, increase their invasiveness, and inhibit apoptosis, such as HOTAIR1, MALAT1 and PVT1, function as oncogenes in non-small cell lung cancer. These lncRNAs are upregulated in NSCLC and promote growth, proliferation, and invasion [26–28]. CBR3-AS1 is highly expressed and functions as an oncogene in many cancer types [9–11, 29–32]. For example, CBR3-AS1 expression is significantly increased in hepatocellular carcinoma and is correlated with tumor size, vascular invasion, and advanced TNM stage, and may be an independent indicator of poor prognosis [11]. CBR3-AS1 expression is significantly increased in colon cancer tissues and cell lines, and is correlated with the depth of invasion, lymph node metastasis, and TNM stage [31]. CBR3-AS1 expression is significantly upregulated in retinoblastoma tissue and cell lines, and correlated with disease progression [29]. CBR3-AS1 is also highly expressed in osteosarcoma tissue and cell lines, and associated with Enneking stage, distant metastasis, histologic grade, and prognosis [10]. CBR3-AS1 expression is also significantly increased in glioma tissue and cell lines compared to adjacent non-cancerous tissues and normal cells, and correlated with shorter OS and PFS [30]. In contrast, the CBR3-AS1 levels in breast cancer tissues and serum are significantly lower than those of healthy tissues and controls [32]. These findings indicate that CBR3-AS1 has regulatory functions that may differ among cancer types. Our bioinformatics analysis results also suggested that CBR3-AS1 expression varied among specific cancers. In addition, our research suggested that CBR3-AS1 was highly expressed in NSCLC, and is higher in patients with malignant phenotypes. Our experimental results showed that CBR3-AS1 could inhibit NSCLC apoptosis, and promote cell proliferation, and promote NSCLC cellular transition into the mitosis stage (G2-M). Moreover, our murine xenograft model demonstrated that CBR3-AS1 overexpression promoted in vivo NSCLC cell growth and proliferation. These results are consistent with other reports that implicate CBR3-AS1 as a cancer gene in NSCLC.

CeRNA regulatory mechanisms mediated by lncRNAs have recently become a major research focus. The ceRNA hypothesis was introduced by Professor Pandolfi in 2011 [33]. Endogenous RNAs, such as mRNA, lncRNA, and pseudogenes, which contain the same miRNA binding sites, may inhibit miRNA attachment to target genes through competitive binding, obviating the silencing effect of miRNA on its target gene. This hypothesis has been confirmed in many important biological processes, such as tumorigenesis, which suggests that lncRNAs in NSCLC can bind to miRNAs in a targeted manner, thus preventing miRNAs from regulating target genes and their corresponding pathways.

MiRNAs silence mRNAs by pair-binding with the 3' UTR region of the target sequence, while lncRNAs affect microRNA-induced gene silencing through binding with miRNA response elements [33]. Qu R et al. found that ZEB1-AS1 was upregulated in NSCLC cells, and that the upregulated ZEB1-AS1 negatively regulated miR-409-3p through the mechanism of ceRNA, thereby affecting the expression and function of its target gene ZEB1 [34]. LncRNA CASC11 is highly expressed in lung cancer tissues and can promote lung cancer development by combining with miRNA-302 to upregulate CDK1 protein expression [35]. Our study found that in NSCLC, cytoplasmic CBR3-AS1 functioned as a ceRNA to provide an oncogenic microenvironment. Moreover, our bioinformatics analysis suggested that CBR3-AS1 and miR-409-3p attached at specific binding sites, and their expressions in NSCLC cells were negatively correlated, suggesting that both might exert regulatory functions through ceRNA-based mechanisms. Our dual luciferase reporter gene experiment confirmed that CBR3-AS1 and miR-409-3p could combine, and our qRT-PCR results confirmed their mutual inhibitory effect.

By evaluating miR-409-3p expression in NSCLC tissue from 48 patients, we found that miR-409-3p was significantly lower in NSCLC cells, and that low miR-409-3p expression was associated with higher tumor stages and worse prognosis. These findings suggested that miR-409-3p might function as a cancer suppressor in NSCLC, which is consistent with the results reported by Qu R et al. [36]. Previous studies have reported that miR-409-3p can inhibit breast cancer by downregulating Akt1 [37]. Wu et al. also confirmed that miR-409-3p can function as a tumor suppressor gene in osteosarcoma by downregulating ZEB1 expression [38]. miR-409-3p may also delay the proliferation of tongue squamous cell carcinoma by inhibiting RDX, thus reducing migration and invasion [39]. Our results indicated that miR-409-3p was poorly expressed in NSCLC, and that miR-409-3p could inhibit CBR3-AS1 expression in NSCLC, thus antagonizing the CBR3-AS1-mediated promotion of proliferation and invasion. In another word, CBR3-AS1 can function as a ceRNA in NSCLC by binding miR409-3p.

SOD1 overexpression can promote cell cycling and inhibit apoptosis, thus accelerating tumor proliferation and metastasis. In addition, our previous results confirmed that SOD1 was one of the target genes of miR-409-3p and its function in NSCLC is regulated by miR-409-3p [18]. miR-409-3p mimic reduced the mRNA and protein expressions of SOD1 in NSCLC cells, SOD1 expression in CBR3-AS1 + miR-409-3p mimic was reserved, indicating that CBR3AS-1 expression antagonized the inhibitory effect of miR-409-3p on SOD1 expression. In contrast, reduced CBR3-AS1 expression could reverse the promotion of SOD1 by an miR-409-3p inhibitor. These results indicate that CBR3-AS1 can combine competitively with miR-409-3p as a ceRNA to regulate the expression of its target gene SOD1 in NSCLC.

Radiotherapy plays a vital role in the treatment of NSCLC. Consequently, the enhancement of NSCLC radiosensitivity is imperative. Previous studies have confirmed that lncRNA could affect the radiosensitivity of various cancer cell types through the mechanism of ceRNA [40]. Wang et al. found that inhibiting PVT1 expression might improve the radiosensitivity of NSCLC through the miR-424-5p/PVT1/CARM1 signaling pathway [40–42]. LincRNA ROR can reduce DNA repair capacity through the LincRNA-ROR/miR-145/Rad18 pathway, thereby enhancing the radiosensitivity of hepatoma cells [41]. Elevated GAS5 increases RECC expression by downregulating miR-21, and accelerates the apoptosis of esophageal squamous cell carcinoma cells after radiotherapy, thus improving radiosensitivity [42]. Therefore, we hypothesized that CBR3-AS1 could affect the radiosensitivity of NSCLC cells through the CBR3-AS1/miR-4093p/SOD1 pathway. Our results confirmed that in NSCLC cells after irradiation, CBR3-AS1 knockdown promotes apoptosis and thereby decreases radioresistance, Furthermore, CBR3-AS1 can regulate miR-409-3p levels, and thereby influence the SOD1 expression after radiotherapy. In addition, our clone forming assay results also showed that CBR3-AS1 expression could eliminate the miR-409-3p-mediated inhibition of SOD1 upregulation and radioresistance. The accumulation of ROS caused by radiotherapy is the primary determinant of radiosensitivity [43]. SOD1 expression can significantly reduce ROS accumulation after radiotherapy, thereby attenuating the ROS-induced cascade that ends in apoptosis [42]. Based on our results combined with those of other studies, it is reasonable to conclude that CBR3-AS1 knockdown can inhibit SOD1 expression in NSCLC cells after radiotherapy through the CBR3-AS1/miR-409-3p/SOD1 pathway, thus leading to ROS accumulation and thereby enhancing radiosensitivity.

DNA repair capacity is also an important determinant of radiosensitivity. The lncRNA-mediated alteration of DNA repair capacity has been the focus of radiosensitivity research in recent years. PVT1knockdown can induce apoptosis of nasopharyngeal carcinoma cells after radiotherapy by affecting the DNA repair pathway [44]. Wang et al. found that lncRNA-LINP1 knockdown may affect Ku80 and DNA-PKs protein expressions and delay the repair of DNA double-strand breaks after radiotherapy, thus increasing apoptosis after ionizing radiation. Our study also found that CBR3-AS1 knockdown increased γH2AX foci significantly and also promoted apoptosis after irradiation, suggesting that apoptosis was accelerated by impaired DNA repair capacity.

Conclusions

lno summary, we proved that CBR3-AS1 is highly expressed in NSCLC cells and tissues through both bioinformatics analysis and empirical data, and that CBR3-AS1 can function as a ceRNA of miR-409-3p to promote NSCLC proliferation and invasion, inhibit apoptosis, and inhibit radiosensitivity through the CBR3-AS1/miR-409-3p/SOD1 pathway (Fig. 7E).

Abbreviations

lncRNAs: Long noncoding RNAs

NSCLC: non-small lung cancer

qRT-PCR: quantitative real-time polymerase chain reaction

ceRNA: competing endogenous RNA

SCLC: small cell lung cancer

OS: overall survival

miRNAs: MicroRNAs

3' UTR: 3' end of the translation sections of target mRNAs

SOD: Superoxide dismutase

DCFH-DA: 2, 7-dichlorofluoresce yellow diacetate

DSBs: DNA double-stranded breaks

PE: Platting efficiency

SF: Survival fraction

Declarations

Ethics approval and consent to participate

All Procedures performed in studies involving human participants or animals were approved by the Ethics Committee of Harbin Medical University Cancer Hospital, Harbin, China. All patients gave their written consent before inclusion in the study.

Consent for publication

Not applicable.

Availability of data and material

All data used or analyzed in this study are all included in the article.

Competing interests

The authors declare that they have no competing interests.

Funding

This work was supported by the Hai Yan Fund of The Third Affiliated Hospital of Harbin Medical University, Harbin, China (number: JJMS2021-05) and the Fundamental Research Funds for the Provincial Universities (number: 2020-KYYWF-1464).

Authors' contributions

SLL and NZ carried out the study and wrote the manuscript. SLL, NZ, CZG and PX helped most of the experiments. NZ, PX and SYW contributed to verify the results and revise the manuscript. SQP and SWJ participated in radiosensitivity test. HW contributed to statistical analysis. All authors read the manuscript and approved the final version.

Acknowledgments

We wish to thank all participants and investigators for their participation of the study.

Authors' information

Department of Thoracic Radiation Oncology, Harbin Medical University Cancer Hospital, Harbin, China.

Shilong Liu and Siyu Wang

Department of Radiation Oncology, Xiang’an Hospital of Xiamen University, Xiamen, China.

Ning Zhan and Piao Xu

Department of Oncology, The First Affiliated Hospital of Harbin Medical University, Harbin, China.

Chunzi Gao

School of Ophthalmology & Optometry and Eye Hospital, School of Biomedical Engineering, Wenzhou Medical University, Wenzhou, China.

Hong Wang

Radiology Technology Center, Harbin Medical University Cancer Hospital, Harbin, China

Shiqi Piao and Suwei Jing

References

1. Siegel RL, Miller KD, Jemal A, Cancer statistics, 2018, CA Cancer J Clin. 68 (2018) 7–30. doi: 10.3322/caac.21442.
2. Esteller M. Non-coding RNAs in human disease. Nat Rev Genet. 2011;12:861–74. doi. 10.1038/nrg3074.
3. Fang Y, Fullwood MJ. Roles, Functions, and Mechanisms of Long Non-coding RNAs in Cancer, Genomics Proteomics Bioinformatics 14 (2016) 42–54. https://doi: 10.1016/j.gpb.2015.09.006.
4. Ayers D, Vandesompele J. Influence of microRNAs and Long Non-Coding RNAs in Cancer Chemoresistance, Genes (Basel). 8 (2017). https://doi: 10.3390/genes8030095.
5. Zhan Y, Zang H, Feng J, et al. Long non-coding RNAs associated with non-small cell lung cancer. Oncotarget. 2017;8:69174–84. doi. 10.18632/oncotarget.20088.
6. Fang Z, Xu C, Li Y, et al. A feed-forward regulatory loop between androgen receptor and PlncRNA-1 promotes prostate cancer progression. Cancer Lett. 2016;374:62–74. doi. 10.1016/j.canlet.2016.01.033.
7. Jin Y, Cui Z, Li X, et al. Upregulation of long non-coding RNA PlncRNA-1 promotes proliferation and induces epithelial-mesenchymal transition in prostate cancer. Oncotarget. 2017;8:26090–9. doi. 10.18632/oncotarget.15318.
8. Cui Z, Ren S, Lu J, et al. The prostate cancer-up-regulated long noncoding RNA PlncRNA-1 modulates apoptosis and proliferation through reciprocal regulation of androgen receptor. Urol Oncol. 2013;31:1117–23. doi. 10.1016/j.urolonc.2011.11.030.
9. Wang CM, Wu QQ, Li SQ, et al., Upregulation of the long non-coding RNA PlncRNA-1 promotes esophageal squamous carcinoma cell proliferation and correlates with advanced clinical stage, Dig Dis Sci 59 (2014) 591–7. https://doi: 10.1007/s10620-013-2956-7.
10. Zhang Y, Meng W, Cui H. LncRNA CBR3-AS1 predicts unfavorable prognosis and promotes tumorigenesis in osteosarcoma, Biomed Pharmacother. 102 (2018) 169–74. https://doi: 10.1016/j.biopha.2018.02.081.
11. Dong L, Ni J, Hu W, et al. Upregulation of Long Non-Coding RNA PlncRNA-1 Promotes Metastasis and Induces Epithelial-Mesenchymal Transition in Hepatocellular Carcinoma. Cell Physiol Biochem. 2016;38:836–46. doi. 10.1159/000443038.
12. Lu J, Clark AG. Impact of microRNA regulation on variation in human gene expression. Genome Res. 2012;22:1243–54. doi. 10.1101/gr.132514.111.
13. Wu KL, Tsai YM, Lien CT, et al., The Roles of MicroRNA in Lung Cancer, Int J Mol Sci 20 (2019). https://doi:10.3390/ijms20071611.
14. Altuvia Y, Landgraf P, Lithwick G, et al. Clustering and conservation patterns of human microRNAs. Nucleic Acids Res. 2005;33:2697–706. doi. 10.1093/nar/gki567.
15. Homami A, Ghazi F. MicroRNAs as biomarkers associated with bladder cancer. Med J Islam Repub Iran. 2016;30:475.

16. Creighton CJ, Gibbons DL, Kurie JM. The role of epithelial-mesenchymal transition programming in invasion and metastasis: a clinical perspective. Cancer Manag Res. 2013;5:187–95. doi. 10.2147/cmar.s35171.
17. Wan L, Zhu L, Xu J, et al. MicroRNA-409-3p functions as a tumor suppressor in human lung adenocarcinoma by targeting c-Met. Cell Physiol Biochem. 2014;34:1273–90. doi. 10.1159/000366337.
18. Liu S, Li B, Xu J, et al. SOD1 Promotes Cell Proliferation and Metastasis in Non-small Cell Lung Cancer via an miR-409-3p/SOD1/SETDB1 Epigenetic Regulatory Feedforward Loop. Front Cell Dev Biol. 2020;8:213. doi. 10.3389/fcell.2020.00213.
19. Tsang CK, Liu Y, Thomas J, et al. Superoxide dismutase 1 acts as a nuclear transcription factor to regulate oxidative stress resistance. Nat Commun. 2014;5:3446. doi. 10.1038/ncomms4446.
20. Brasil AA, de Carvalho MDC, Gerhardt E, et al. Characterization of the activity, aggregation, and toxicity of heterodimers of WT and ALS-associated mutant Sod1. Proc Natl Acad Sci U S A. 2019;116:25991–6000. doi. 10.1073/pnas.1902483116.
21. Somwar R, Erdjument-Bromage H, Larsson E, et al. Superoxide dismutase 1 (SOD1) is a target for a small molecule identified in a screen for inhibitors of the growth of lung adenocarcinoma cell lines. Proc Natl Acad Sci U S A. 2011;108:16375–80. doi. 10.1073/pnas.1113554108.
22. Glasauer A, Sena LA, Diebold LP, et al. Targeting SOD1 reduces experimental non–small-cell lung cancer. J Clin Invest. 2014;124:117–28. doi. 10.1172/jci71714.
23. Macedo-Silva C, Miranda-Gonçalves V, Henrique R, et al., The Critical Role of Hypoxic Microenvironment and Epigenetic Deregulation in Esophageal Cancer Radioresistance, Genes (Basel). 10 (2019). doi: 10.3390/genes10110927.
24. Spangler R, Goddard NL, Spangler DN, et al. Tests of the single-hit DNA damage model. J Mol Biol. 2009;392:283–300. doi. 10.1016/j.jmb.2009.07.012.
25. Gutschner T, Hämmerle M, Eissmann M, et al. The noncoding RNA MALAT1 is a critical regulator of the metastasis phenotype of lung cancer cells. Cancer Res. 2013;73:1180–9. doi. 10.1158/0008-5472.can-12-2850.
26. Cui D, Yu CH, Liu M, et al., Long non-coding RNA PVT1 as a novel biomarker for diagnosis and prognosis of non-small cell lung cancer, Tumour Biol 37 (2016) 4127–34. https://doi: 10.1007/s13277-015-4261-x.
27. Liu Z, Sun M, Lu K, et al., The long noncoding RNA HOTAIR contributes to cisplatin resistance of human lung adenocarcinoma cells via downregualtion of p21(WAF1/CIP1) expression, PLoS One. 8 (2013) e77293. doi: 10.1371/journal.pone.0077293.
28. Derrien T, Johnson R, Bussotti G, et al. The GENCODE v7 catalog of human long noncoding RNAs: analysis of their gene structure, evolution, and expression. Genome Res. 2012;22:1775–89. doi. 10.1101/gr.132159.111.
29. Wang S, Liu J, Yang Y, et al., PlncRNA-1 is overexpressed in retinoblastoma and regulates retinoblastoma cell proliferation and motility through modulating CBR3, IUBMB Life. 70 (2018) 969–

975. doi: 10.1002/iub.1886.

30. Wang X, Yan Y, Zhang C, et al. Upregulation of lncRNA PlncRNA-1 indicates the poor prognosis and promotes glioma progression by activation of Notch signal pathway. Biomed Pharmacother. 2018;103:216–21. doi. 10.1016/j.biopha.2018.03.150.
31. Song W, Mei JZ, Zhang M. Long Noncoding RNA PlncRNA-1 Promotes Colorectal Cancer Cell Progression by Regulating the PI3K/Akt Signaling Pathway. Oncol Res. 2018;26:261–8. doi. 10.3727/096504017x15031557924132.
32. Baratieh Z, Khalaj Z, Honardoost MA, et al. Aberrant expression of PlncRNA-1 and TUG1: potential biomarkers for gastric cancer diagnosis and clinically monitoring cancer progression. Biomark Med. 2017;11:1077–90. doi. 10.2217/bmm-2017-0090.
33. Salmena L, Poliseno L, Tay Y, et al. A ceRNA hypothesis: the Rosetta Stone of a hidden RNA language? Cell. 2011;146:353–8. doi. 10.1016/j.cell.2011.07.014.
34. Shi X, Sun M, Liu H, et al. Long non-coding RNAs: a new frontier in the study of human diseases. Cancer Lett. 2013;339:159–66. doi. 10.1016/j.canlet.2013.06.013.
35. Qu R, Chen X, Zhang C. LncRNA ZEB1-AS1/miR-409-3p/ZEB1 feedback loop is involved in the progression of non-small cell lung cancer. Biochem Biophys Res Commun. 2018;507:450–6. doi. 10.1016/j.bbrc.2018.11.059.
36. Tong W, Han TC, Wang W, et al. LncRNA CASC11 promotes the development of lung cancer through targeting microRNA-302/CDK1 axis. Eur Rev Med Pharmacol Sci. 2019;23:6539–47. doi. 10.26355/eurrev_201908_18539.
37. Zhang G, Liu Z, Xu H, et al. miR-409-3p suppresses breast cancer cell growth and invasion by targeting Akt1. Biochem Biophys Res Commun. 2016;469:189–95. doi. 10.1016/j.bbrc.2015.11.099.
38. Wu L, Zhang Y, Huang Z, et al. MiR-409-3p Inhibits Cell Proliferation and Invasion of Osteosarcoma by Targeting Zinc-Finger E-Box-Binding Homeobox-1. Front Pharmacol. 2019;10:137. doi. 10.3389/fphar.2019.00137.
39. Chen H, Dai J. miR-409-3p suppresses the proliferation, invasion and migration of tongue squamous cell carcinoma via targeting RDX. Oncol Lett. 2018;16:543–51. doi. 10.3892/ol.2018.8687.
40. Wang D, Hu Y. Long Non-coding RNA PVT1 Competitively Binds MicroRNA-424-5p to Regulate CARM1 in Radiosensitivity of Non-Small-Cell Lung Cancer. Mol Ther Nucleic Acids. 2019;16:130–40. doi. 10.1016/j.omtn.2018.12.006.
41. Chen Y, Shen Z, Zhi Y, et al. Long non-coding RNA ROR promotes radioresistance in hepatocelluar carcinoma cells by acting as a ceRNA for microRNA-145 to regulate RAD18 expression. Arch Biochem Biophys. 2018;645:117–25. doi. 10.1016/j.abb.2018.03.018.
42. Lin J, Liu Z, Liao S, et al. Elevation of long non-coding RNA GAS5 and knockdown of microRNA-21 up-regulate RECK expression to enhance esophageal squamous cell carcinoma cell radio-sensitivity after radiotherapy. Genomics. 2020;112:2173–85. doi. 10.1016/j.ygeno.2019.12.013.
43. Xu Z, Zhang Y, Ding J, et al. miR-17-3p Downregulates Mitochondrial Antioxidant Enzymes and Enhances the Radiosensitivity of Prostate Cancer Cells. Mol Ther Nucleic Acids. 2018;13:64–77. doi.

10.1016/j.omtn.2018.08.009.

44. He Y, Jing Y, Wei F, et al., Long non-coding RNA PVT1 predicts poor prognosis and induces radioresistance by regulating DNA repair and cell apoptosis in nasopharyngeal carcinoma, Cell Death Dis 9 (2018) 235. https://doi: 10.1038/s41419-018-0265-y.

Figures

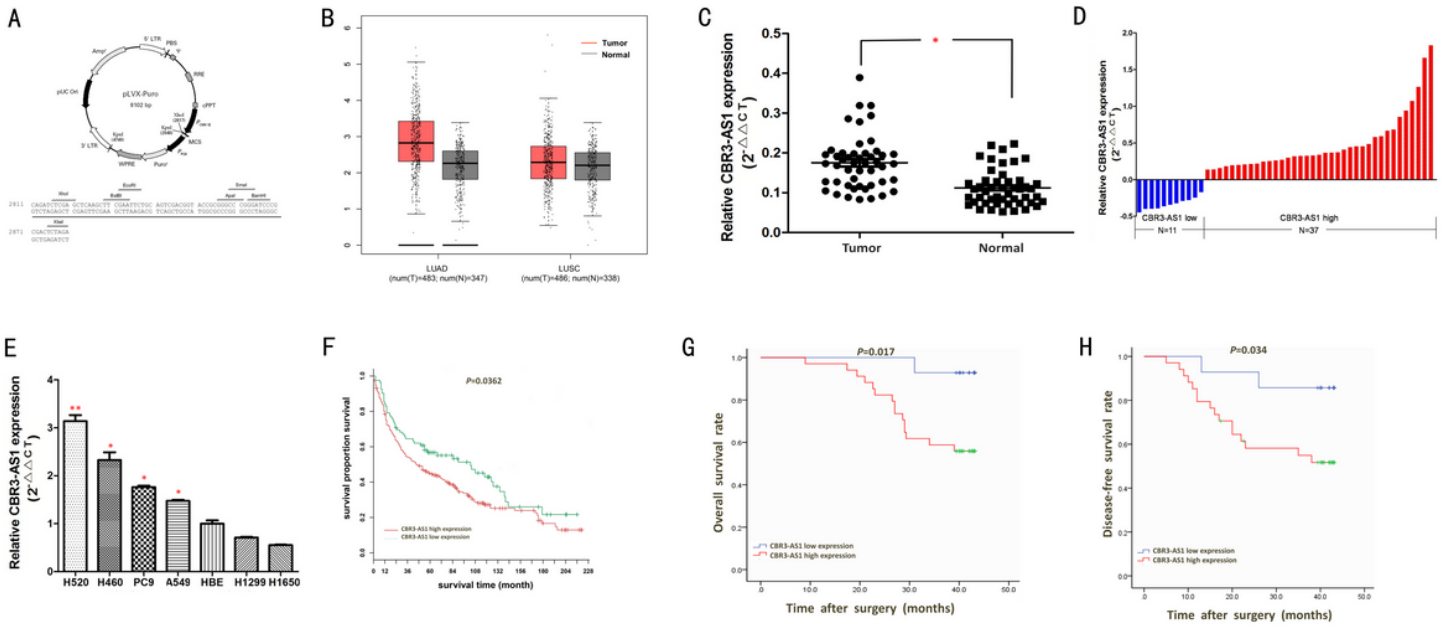

Figure 1

The expression of CBR3-AS1 and its relationship with prognosis. (A). Structural sketch of Lentiviral expression vector. (B).CBR3-AS1 expression is higher in lung adenocarcinoma and lung squamous cell carcinoma than in normal tissues; (C). CBR3-AS1 expression in cancer tissues of NSCLC patients was significantly higher than that in adjacent normal tissues; (D). the proportion of CBR3-AS1 high expression in patients was significantly higher than that of lower expression; (E). CBR3-AS1 in NSCLC cell line and human normal bronchial epithelium expression in cell lines; (F). CBR3-AS1 high expression group has lower survival rate than low expression group; (G-H). The OS and DFS in the group of CBR3-AS1 high expression were both inferior to those in the CBR3-AS1 low expression group. *P<0.05, **P<0.01.

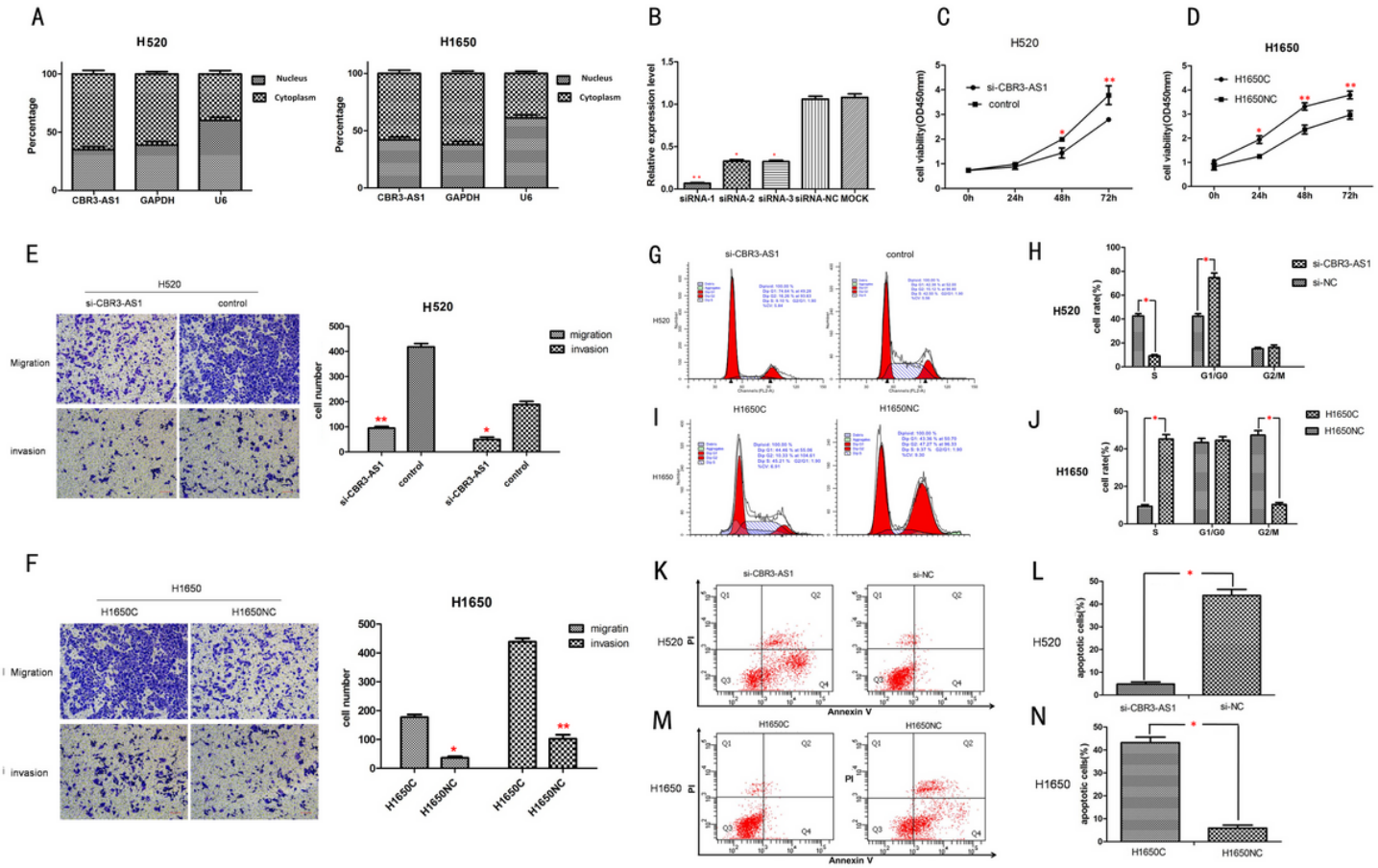

Figure 2

Regulation of NSCLC cell proliferation, invasion, metastasis, apoptosis, and the cell cycle by CBR3-AS1. (A). CBR3-AS1 is mainly expressed in the cytoplasm of NSCLC; (B). siRNA-1 knocks down CBR3-AS1 most efficiently; (C–D). Proliferation of H520 and H1650 cells analyzed by CCK-8 assay after inhibition or overexpression of CBR3-AS1. (E–F). Evaluation of H520 and H1650 cell migration and invasion by transwell assay after inhibited or overexpressed of CBR3-AS1. (G–N). Measurement of apoptosis and the cell cycle by flow cytometryin cells with upregulated or downregulated CBR3-AS1 expression. Experiments were conducted using triplicate samples and each experiment was conducted three times; *P<0.05, **P<0.01.

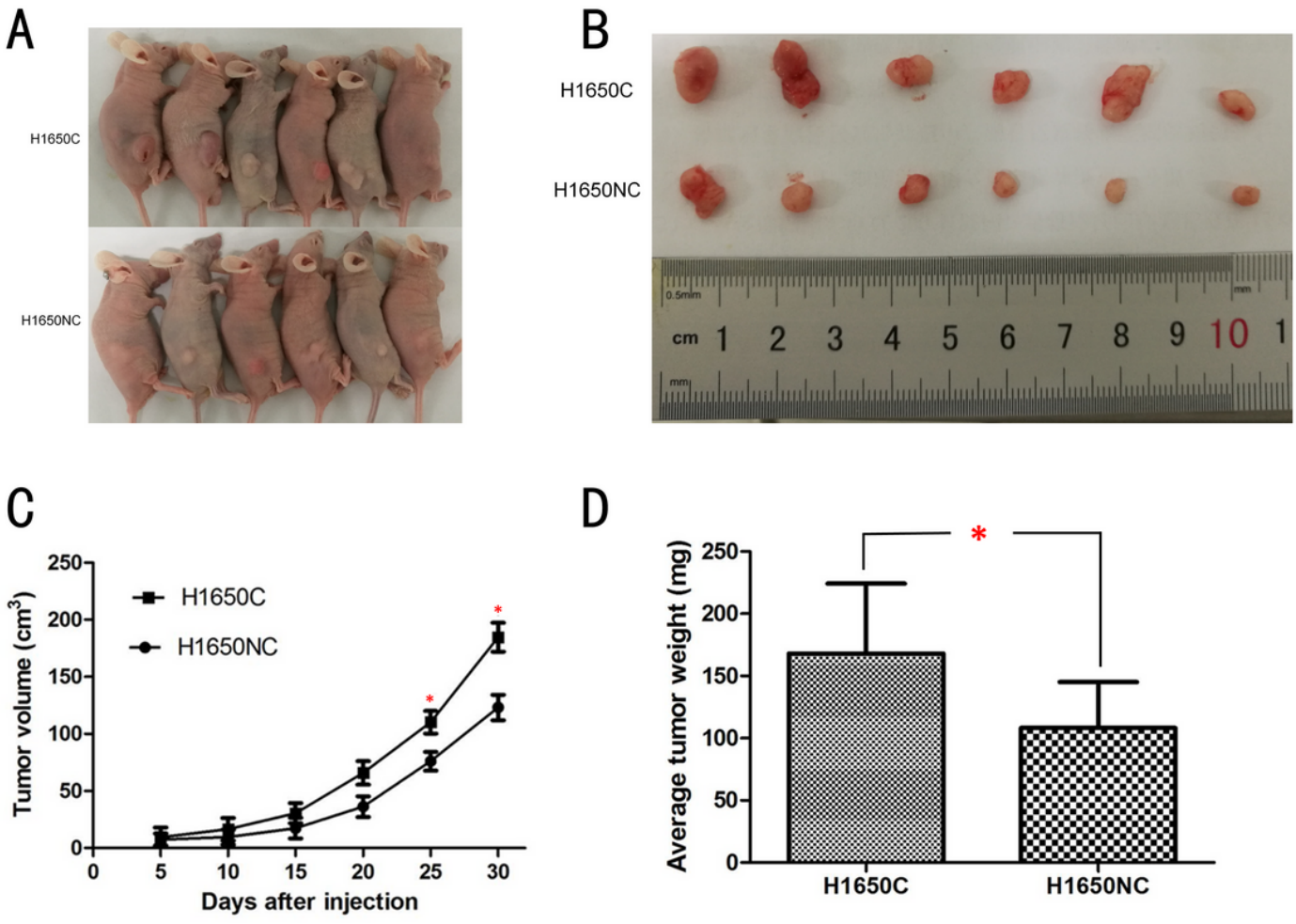

Figure 3

The impact of CBR3-AS1 on tumorigenesis in vivo. (A-B). Representative images of Subcutaneous injection of H1650C and H1650NC cells in nude mice; (C-D). Compared with the control group, the tumor volume and tumor volume in nude mice were significantly increased after CBR3-AS1 overexpression. Tumor volumes were calculated after injection every three days Tumor weights are represented as means of tumor weights ± SD (n = 12). *P<0.05.

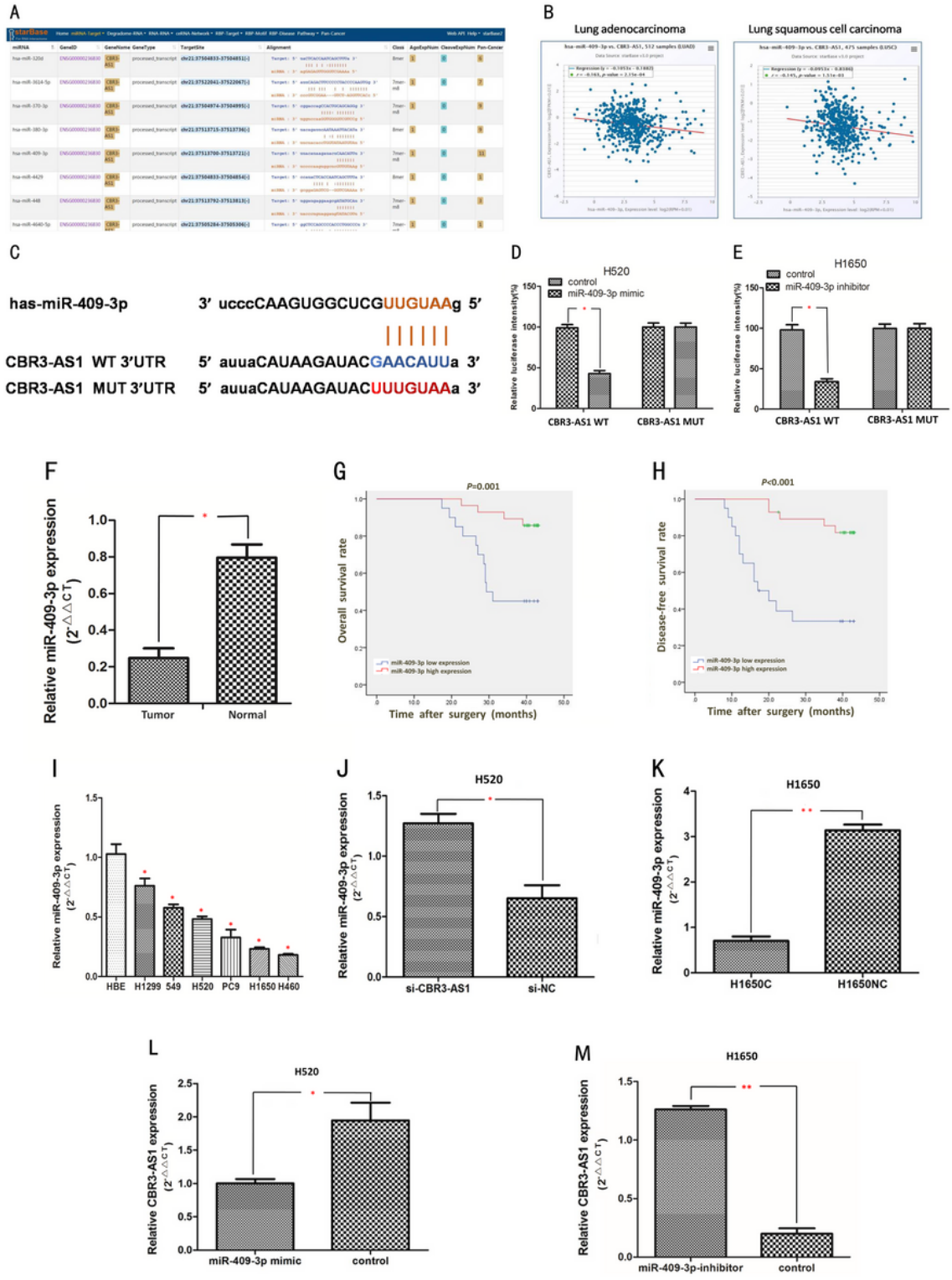

Figure 4

The interaction of CBR3-AS1 and miR-409-3p. (A). Some microRNAs that may interact with CBR3-AS1 predicted using the starBasev3.0. (B). Relationship between the expression of CBR3-AS1 and miR-409-3p level in starBasev3.0. (C). Binding sites for CBR3-AS1 in miR-409-3p squences predicted using the starBasev3.0 are shown. (D-E). Dual-luciferase reporter gene assay to determine luciferase activity from wild-type (WT) or mutant CBR3-AS1 sequences 48h after transfection. (F). qRT-PCR showing that miR-

409-3p expression was inhibited in NSCLC tissue and cells. (G-H). the OS and DFS of patients with high or low miR-409-3p expression. (I). miR-409-3p expression in multiple NSCLC cell lines compared to normal human epithelial cells. (J-K). Relative expression of miR-409-3p in NSCLC cells with si-CBR3-AS1 or with pLVX-puro-CBR3-AS1(H1650C). (L-M). Relative CBR3-AS1 expression in NSCLC cells transfected with miR-409-3p inhibitor or miR-409-3p mimic. Each experiment was conducted in triplicate; *P<0.05, **P<0.01.

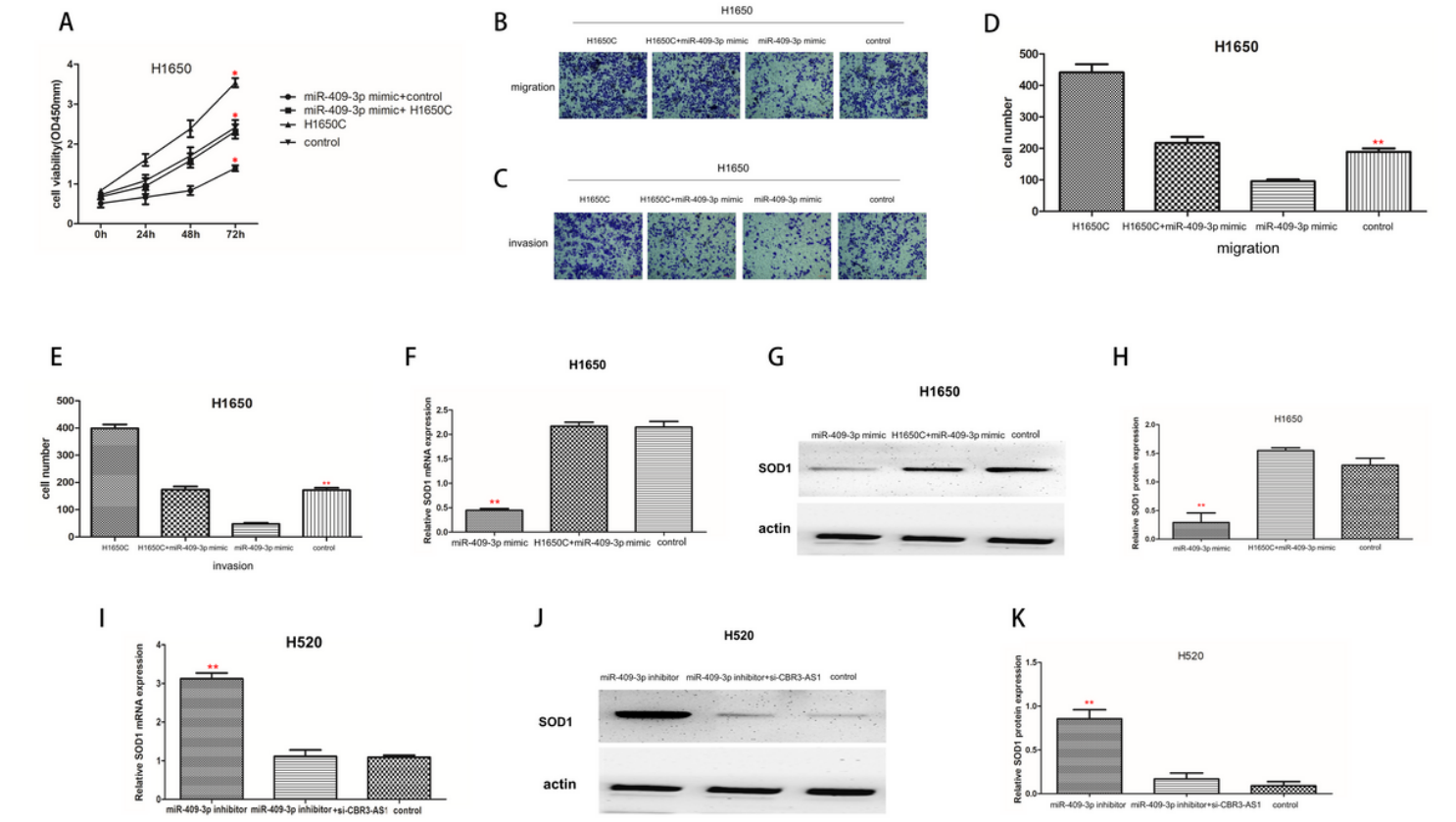

Figure 5

Effect of miR-409-3p on the function of CBR3-AS1 in NSCCLC cells. (A). The effects of CBR3-AS1 on proliferation of NSCLC cells was rescued by miR-409-3p mimic; (B-E). The effects of CBR3-AS1 on invasion and migration of NSCLC cells was also rescued by miR-409-3p mimic. (F-H).CBR3-AS1 overexpression can relieve the inhibition of miR-409-3p on SOD1 mRNA and protein expression; (I-K). Reduction of CBR3-AS1 expression can reverse miR-409-3p inhibitor's role in promoting SOD1 mRNA and protein expression.

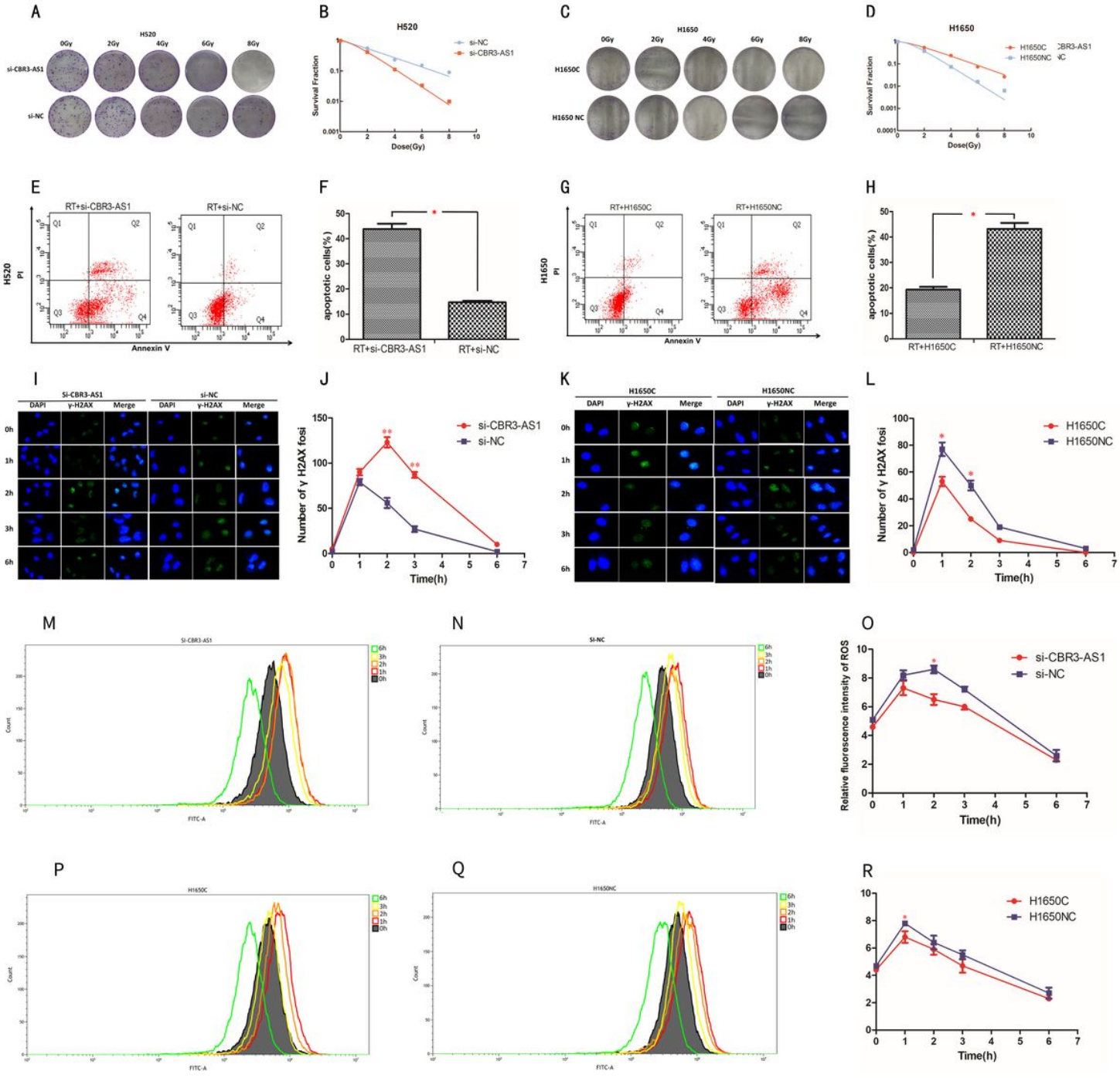

Figure 6

Effect of CBR3-AS1 expression on radiosensitivity of NSCLC cells. (A). Clone formation of H520 cells after knockdown of CBR3-AS1 by different doses of X-ray irradiation; (B). Cell survival curves of Corresponding group cells were carried out with single-hit multi-target model in H520 cells. (C). Clone formation of H1650 cells after overexpression of CBR3-AS1 by different doses of X-ray irradiation; (D). Cell survival curves of Corresponding group cells were carried out with single-hit multi-target model in H1650 cells. (E-F). Compared with the control group, the apoptosis rate of RT+si-CBR3-AS1 group was significantly increased; (G-H). In contrast, the apoptosis rate of H1650 cells overexpressing CBR3-AS1

was significantly lower than that of the control group after radiotherapy. (I-J).Effects of knockdown of CBR3-AS1 on focal formation of γH2AX in NSCLC cells at different time point.(K-L). Effects of CBR3-AS1 overexpression at different time points on focal formation of γH2AX in NSCLC cells. Blue: nuclear staining; green: γH2AX staining; ROS expression was significantly increased in the si-CBR3-AS1 group, gradually rising to peak at approximately 2h post-irradiation, followed by a gradual reduction, and significantly exceeding the results of the control group at corresponding time points (Fig. 6M-O). The ROS in H1650C group peaked at 1h after ionizing radiation and then gradually decreased. The ROS expression levels at each time point were significantly reduced compared with the control group (Figs. 6P-R). *P<0.05, **P<0.01.

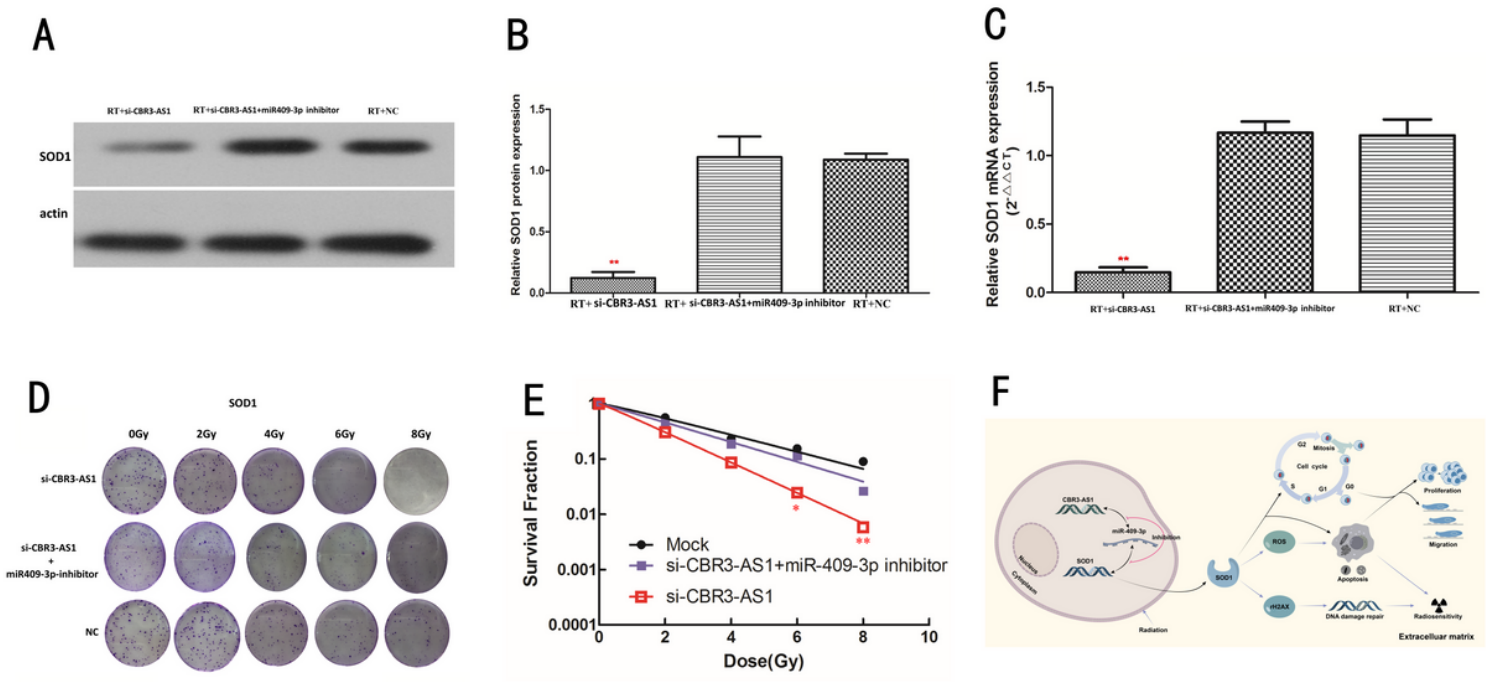

Figure 7

CBR3-AS1 regulates SOD1 expression through miR-409-3p and affects radiosensitivity of NSCLC cells. (A-C). CBR3-AS1 affects SOD1 expression after radiotherapy by regulating miR-409-3p; (D-E). CBR3-AS1 / miR-409-3p / SOD1 affects radiosensitivity of NSCLC cells. (F). The mechanism of CBR3-AS1/miR-409-3p/SOD1 in NSCLC.